Phased Array Calibration

Ron Sorace, *Senior Member, IEEE*

***Abstract*—Calibration of a phased array antenna while the antenna is in service can be a complex and time-consuming procedure that affects use of the antenna and imposes an unacceptable overhead on the system. The procedure described herein uses a maximum likelihood algorithm to minimize the number of measurements, thus reducing the impact on the system and shifting the overhead to a remote site.**

***Index Terms*—Antenna measurements, calibration, phased array calibration.**

I. Introduction

A PLANAR phased array antenna as depicted in Fig. 1 consists of an array of $M \times N$ elements for transmission or reception of radiation. The radiating elements are fed with one or more signals whose amplitudes and phases are determined to form a beam in a specified direction. In Fig. 1, for example, three signals are fed to or received from each radiating element. The signal at each element is the sum of the three signals with phase shifting and attenuation dictated by the desired direction of the beam for each of the radiated signals.

Since accurate pointing of a beam of a phased array antenna demands precise control of phase and amplitude, exact knowledge of the gain and phase of the electronics is essential. However, the parameters of electronic components vary with temperature and can drift over time. Hence, periodic calibration of a phased array may be necessary to ascertain phase and amplitude corrections for each element. Calibration may be performed by pointing an unused beam of the array at a fixed location and transmitting or receiving signals that permit calibration of individual elements. Performance of the calibration in a closed-loop mode may be desirable to conserve power or contain processing complexity for systems such as arrays on satellites. For example, a transmit array may be calibrated by sending a signal to the station, but the signal may have originated at the station. Similarly, a receive array may be calibrated by receiving a signal from the station, and the signal may be returned to the station. To calibrate the entire array, the procedure must be repeated for each element of the array. Note that pointing a beam at a fixed station assumes that dependence of calibration on direction is negligible. If parameters are sensitive to pointing direction, then an alternative such as multiple stations must be implemented.

To calibrate a beam for a single element of an array, the phases of all elements for that beam are set to the current corrected phase state for pointing the beam at the fixed station. The settings for this beam position are regarded as the 0° state. Typically, the phase corresponding to the beam for the element being calibrated is cycled through all possible phase settings [1], and the received or transmitted power is measured at each setting. Repetition of the cycle allows the receiver at the fixed terminal to integrate multiple measurements of the power to improve the signal-to-noise ratio of the measurement. After sufficient data are acquired, the difference between the setting giving maximum power and the assumed 0° setting is taken to be the calibration offset. The procedure is repeated for each element in the array, and the previous phase correction for each element is adjusted based on the detected error. A new correction value is established for each element, and the phase calibration and correction of the array are repeated until the phase errors converge below an acceptable level. The potential impact on the service of the array depends on the number of repetitions, the number of phase settings, and the time for measurement at each setting.

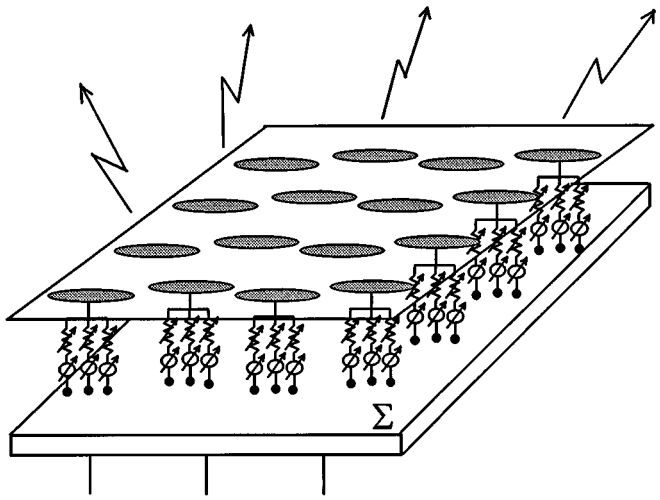

Fig. 1. Phased array antenna with three beams.

The proposed method of calibration reduces the potential overhead by reducing the number of phase settings at which measurements must be performed. Measurements at four orthogonal phase settings [2] yield sufficient information to obtain a maximum likelihood estimate of the calibration offset. To perform calibration, the phases of all elements for a given beam are initialized for pointing at the fixed station as described previously. These settings again constitute the 0° setting. Subsequently, the phase of an element is sequenced through the phase states corresponding to 180°, 90°, and 270° relative to the reference state. The element phase error is calculated from power measurements at the four phase states, and the procedure is repeated for each element in the array. As in the previous approach, additional measurements may be used to improve signal-to-noise ratio, and the procedure can be repeated to achieve desired accuracy within resolution of the phase shifters, since the algorithm is intrinsically convergent.

Manuscript received May 21, 1999; revised September 12, 2000.

The author is with Boeing Space Systems, formerly Hughes Space and Communications Company, Los Angeles, CA 90009 USA.

Publisher Item Identifier S 0018-926X(01)01835-X.

0018–926X/01$10.00 © 2001 IEEE

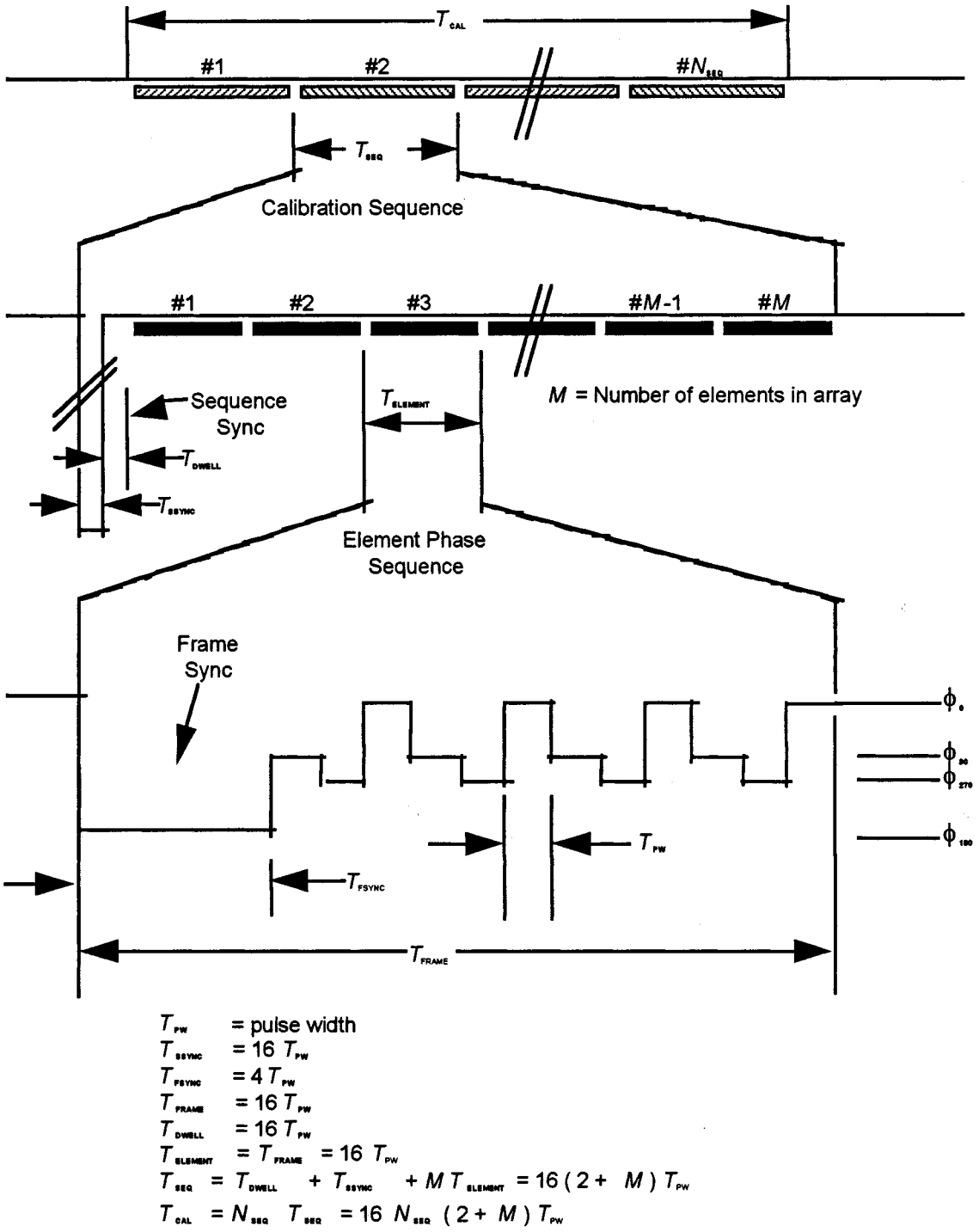

Fig. 2. Array calibration signal structure.

II. Calibration Signal Structure

Fig. 2 illustrates the calibration sequence generated by the array. The sequence, which is repeated N_{SEQ} times, starts with a synchronization time T_{SSYNC} during which the phase of every odd-numbered element is switched by 180° to produce a signal null. This null is followed by a dwell time T_{DWELL} during which all array elements remain at their 0° state and one repetition of the element phase sequence for each element in the array. The individual element phase sequence starts with a synchronization time T_{FSYNC} during which the element remains in its 180° state to mark the beginning of the element transmission. This is followed by repetitions of the calibration frame during which the phase of the element is switched through a phase pattern. The times given in Fig. 2 summarize the timing parameters for the calibration sequence as realized for an application in satellite communications.

The calibration frame pattern is shown at the bottom of Fig. 2 and is constructed to accommodate large phase errors. A phase transition from the 0° state ϕ_0 to the 180° state ϕ_{180} is held for

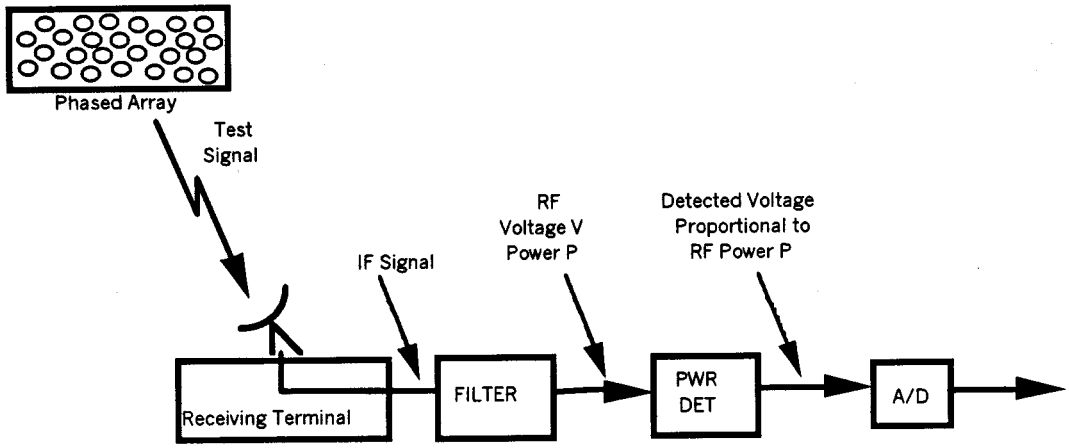

Fig. 3. Measurement block diagram.

a time T_{FSYNC} to provide unambiguous synchronization and a power measurement P_{180} at the receiver. Subsequently, the phase is toggled by 90°, 270°, and 0° between states ϕ_{90}, ϕ_{270}, and ϕ_0 with corresponding power measurements P_{90}, P_{270}, and P_0 being performed.

Special cases occur within the frame pattern when the element phase error δ_k is close to one of four values. When δ_k is approximately either 90° or 270°, P_0 and P_{180} are approximately equal, and the transition from ϕ_0 to ϕ_{180} may not be detected. However, the transition from ϕ_{180} to ϕ_{90} at the end of the frame synchronization will be detected, as will the transitions from ϕ_{270} to ϕ_{180} and from ϕ_{180} to ϕ_{90} at the start of the second repetition of the phase pattern. Similarly, when δ_k is approximately either 45° or 235°, P_{180} and P_{90} are approximately equal, so the transition from ϕ_{180} to ϕ_{90} may not be detected. In this case, the transition from ϕ_0 to ϕ_{180} at the beginning of the long pulse will be detected, as will the same transition at the start of the second repetition of the phase pattern. Thus, the phase pattern can be correctly synchronized in all cases.

III. Signal Detection

As described previously, the calibration signal consists of a sequence of phase transitions to states $\phi_0, \phi_{180}, \phi_{90}$, and ϕ_{270} and with power measurements P_0, P_{180}, P_{90}, and P_{270} performed in each state. The measurement system is depicted in Fig. 3 and consists of a narrow-band filter followed by a quadratic detector whose output voltage is proportional to the power of the radio-frequency (RF) signal. Quadratic detection is preferable to a correlation receiver, which requires carrier recovery that is susceptible to timing variation.

The received voltage at the input to the power detector when all elements are set to their nominal phases can be written

$$r(t) = \sum_{m=1}^{M} a_m \cos(\omega t + \delta_m) + n(t) \tag{1}$$

where

- ω transmitted frequency;
- δ_m phase offset of the mth element relative to its nominal value;
- a_m RF voltage from the mth element;
- $n(t)$ narrow-band thermal noise, which is uncorrelated between samples.

The narrow-band noise is $n(t) = n_c(t)\cos\omega t - n_s(t)\sin\omega t$ where $n_c(t)$ and $n_s(t)$ are the in-phase and quadrature components, respectively. These components are independent and identically distributed Gaussian processes having zero mean and variance $\sigma^2 = N_0 B$ with $N_0/2$ the noise power density and $2B$ the bandwidth of the filter. Introducing a phase of θ on the kth element yields

$$\begin{aligned} r(t) &= \sum_{\substack{m=1 \\ m\neq k}}^{M} a_m \cos(\omega t + \delta_m) + a_k \cos(\omega t + \theta + \delta_k) + n(t) \\ &= \left[\sum_{\substack{m=1 \\ m\neq k}}^{M} a_m \cos\delta_m + a_k \cos(\theta + \delta_k) + n_c(t)\right] \cos\omega t \\ &\quad - \left[\sum_{\substack{m=1 \\ m\neq k}}^{M} a_m \sin\delta_m + a_k \sin(\theta + \delta_k) + n_s(t)\right] \\ &\quad \times \sin\omega t \end{aligned} \tag{2}$$

at the input to the power detector. The output from the power detector is the square of the envelope of its input

$$q = (A_c + v_c + n_c)^2 + (A_s + v_s + n_s)^2 \tag{3}$$

where

$$A_c = \sum_{\substack{m=1 \\ m\neq k}}^{M} a_m \cos\delta_m, \quad A_s = \sum_{\substack{m=1 \\ m\neq k}}^{M} a_m \sin\delta_m,$$
$$v_c = a_k \cos(\theta + \delta_k), \quad \text{and} \quad v_s = a_k \sin(\theta + \delta_k).$$

The output of the power detector is sampled at a time interval $T_s \gg 1/B$ so that the samples are uncorrelated. The sampled output of the power detector is

$$q_\ell = (A_c + v_c + n_{cl})^2 + (A_s + v_s + n_{sl})^2 \tag{4}$$

where the variables $n_{c\ell}$ and $n_{s\ell}$ are Gaussian variables as described previously. For each element, the statistic q_ℓ is a noncen-

tral chi-squared random variable with two degrees of freedom and density

$$p(q_\ell) = (2\sigma^2)^{-1} \exp[-(q_\ell + \lambda)/2\sigma^2] I_0\left(\frac{\sqrt{q_\ell \lambda}}{\sigma^2}\right) \quad (5)$$

with noncentral parameter

$$\lambda = (A_c + v_c)^2 + (A_s + v_s)^2. \quad (6)$$

The mean and variance of the statistic q_ℓ are

$$\mu = E\{q_\ell\} = \lambda + 2\sigma^2 \quad (7)$$
$$\sigma_q^2 = \mathrm{Var}\{q_\ell\} = 4\sigma^2\lambda + 4\sigma^4 \quad (8)$$

respectively, and $I_0(\cdot)$ in (5) denotes the modified Bessel function of the first kind of order zero.

IV. Phase and Amplitude Error Estimation

If L samples of the output of the power detector are averaged to form the statistic

$$\bar{q} = \frac{1}{L}\sum_{\ell=1}^{L} q_\ell \quad (9)$$

with the samples q_ℓ of q being independent, then the statistic $\bar{q}$ is a noncentral chi-squared random variable having $2L$ degrees of freedom with noncentral parameter

$$\bar{\lambda} = \frac{1}{L}\sum_{\ell=1}^{L}[(A_c + v_c)^2 + (A_s + v_s)^2] = \lambda. \quad (10)$$

The density of $\bar{q}$ is

$$p(\bar{q}) = \left(\frac{2\sigma^2}{L}\right)^{-1} \left(\frac{\bar{q}}{\lambda}\right)^{\frac{L-1}{2}} \exp\left[-\frac{\bar{q}+\lambda}{2\sigma^2/L}\right] I_{L-1}\left(\frac{\sqrt{\bar{q}\lambda}}{\sigma^2/L}\right) \quad (11)$$

with mean

$$\bar{\mu} = E\{\bar{q}\} = \mu = E\{q\} = \lambda + 2\sigma^2 \quad (12)$$

and variance

$$\bar{\sigma}^2 = \mathrm{Var}\{\bar{q}\} = (4\sigma^2\lambda + 4\sigma^4)/L. \quad (13)$$

The statistic $\bar{q}$ is an unbiased estimate of μ since

$$E\{\bar{q}\} = \frac{1}{L}\sum_{\ell=1}^{L} E\{q_\ell\} = E\{q\} = \lambda + 2\sigma^2 \quad (14)$$

and it is asymtotically efficient.

Although the tendency might be to seek maximum- likelihood estimates for the phase variation δ_k and the amplitude variation a_k by solving the gradient of the likelihood function, the expression in (14) provides a more immediate approach. The chi-squared distribution is approximately Gaussian about the mean for large degrees of freedom, and the sample mean $\bar{q}$ is asymptotically efficient. From (14), note that $\bar{q}$ is a biased estimate of λ and that λ may be solved for δ_k and a_k from (6) and the expressions for v_c and v_s following (3). The bias in the sample mean may be removed by considering of the differences $\bar{q}_{270} - \bar{q}_{90}$ and $\bar{q}_0 - \bar{q}_{180}$, which are unbiased estimates

$$\bar{q}_{270} - \bar{q}_{90} = 4a_k(A_c \sin\delta_k - A_s \cos\delta_k) \quad (15)$$
$$\bar{q}_0 - \bar{q}_{180} = 4a_k(A_c \cos\delta_k + A_s \sin\delta_k). \quad (16)$$

Note that the element index k is understood for the statistics $\bar{q}$, and the power is measured for each phase setting of each element. Since only the phase of the kth element is varying, the sum of the other element voltages forms the reference, i.e., $A_s \cong 0$, which gives

$$\bar{q}_{270} - \bar{q}_{90} \cong 4a_k A_c \sin\delta_k \quad (17)$$
$$\bar{q}_0 - \bar{q}_{180} \cong 4a_k A_c \cos\delta_k. \quad (18)$$

Hence, the estimates of the phase and amplitude variations become

$$\hat{\delta}_k = \tan^{-1}\left(\frac{\bar{q}_{270} - \bar{q}_{90}}{\bar{q}_0 - \bar{q}_{180}}\right) \quad (19)$$
$$\hat{a}_k = \frac{\sqrt{(\bar{q}_{270} - \bar{q}_{90})^2 + (\bar{q}_0 - \bar{q}_{180})^2}}{4A_c}. \quad (20)$$

The deviations of these estimates are readily derived from first-order differentials

$$\hat{\sigma}_\delta^2 = \mathrm{Var}\{\hat{\delta}_k\} \cong \sum_\theta \left(\frac{\partial\hat{\delta}_k}{\partial\bar{q}_\theta}\right)^2$$
$$\sigma_\theta^2 = \frac{\sigma^2/L}{2a_k^2A_c^2}\left(\sigma^2 + A_c^2 + A_s^2 + a_k^2\right) \quad (21)$$
$$\hat{\sigma}_a^2 = \mathrm{Var}\{\hat{a}_k\} \cong \sum_\theta \left(\frac{\partial\hat{a}_k}{\partial\bar{q}_\theta}\right)^2$$
$$\sigma_\theta^2 = \frac{\sigma^2/L}{2A_c^2}\left(\sigma^2 + A_c^2 + A_s^2 + a_k^2\right). \quad (22)$$

Since the elements are driven approximately equally, $a_m \cong a_k$ for all m and $A_c \cong (M-1)a_k$. Using the approximation $A_s \cong 0$ gives the errors

$$\hat{\sigma}_\delta^2 \cong \frac{N_0B}{4LP_k}\left[1 + \frac{N_0B}{2P_k(M-1)^2}\right]$$
$$\hat{\sigma}_a^2 \cong \frac{N_0B}{2L}\left[1 + \frac{N_0B}{2P_k(M-1)^2}\right] \quad (23)$$

where $P_k = a_k^2/2$ denotes the power of the kth element. The deviation of the phase error estimate $\hat{\sigma}_\delta$ from (23) is plotted in Fig. 4 and indicates that an accuracy of 2° requires approximately 12 iterations at a signal-to-noise power ratio of approximately 13 dB per element.

Since the residual phases of all elements other than the kth were disregarded in (17) and (18) and the subsequent analysis, the estimates of δ_k and a_k are relative to the aggregate of the other elements. Note that this reference varies depending on which element is being tested. Hence, caution must be exercised to update the element corrections only after calibration of the entire array.

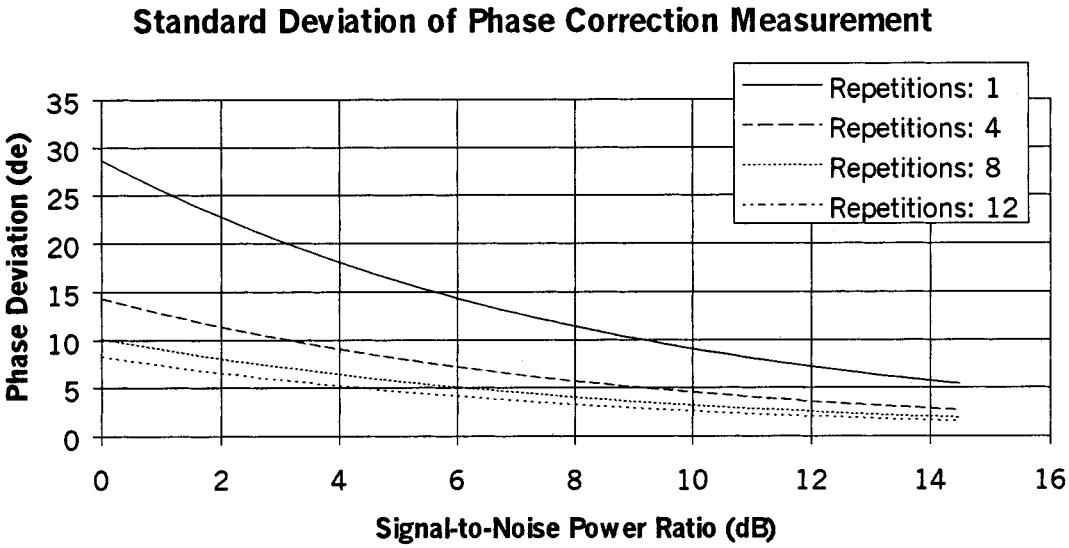

Fig. 4. Error deviation of phase correction.

V. Phase Pattern Detection and Synchronization

The transition in the phase sequence at the initiation of calibration must be immediately detectable to achieve synchronization. A transition in phase from θ to ϕ is detected by comparing the difference $q_\theta - q_\phi$ to a threshold τ, which is set nominally at the midpoint of the range

$$\tau = (q_\theta - q_\phi)/2 \cong 4(M-1)P_k. \tag{24}$$

The probability of this transition's being detected is

$$\begin{aligned} P_{\theta\phi} &= \Pr\{q_\theta - q_\phi > \tau\} \\ &= \int_0^\infty p(q_\phi) \int_{q_\phi+\tau}^\infty p(q_\theta)\, dq_\theta\, dq_\phi. \end{aligned} \tag{25}$$

In particular, the false alarm rate is

$$\begin{aligned} P_{\text{fa}} &= \Pr\{q_\theta - q_\phi > \tau \,|\, \theta = \phi\} \\ &= \int_0^\infty p(q_\theta) \int_{q_\theta+\tau}^\infty p(q'_\theta)\, dq'_\theta\, dq_\theta \end{aligned} \tag{26}$$

and the probility of detection is

$$\begin{aligned} P_D &= \Pr\{q_\theta - q_\phi > \tau \,|\, \theta - \phi = \pi\} \\ &= \int_0^\infty p(q_\phi) \int_{q_\phi+\tau}^\infty p(q_\theta)\, dq_\theta\, dq_\phi \end{aligned} \tag{27}$$

where the noncentral chi-squared density $p(\cdot)$ is given by (5). These integrals are difficult to evaluate, but the variable $q = q_\theta - q_\phi$ may be approximated by a Gaussian distribution with mean $E\{q\} = \lambda_\theta - \lambda_\phi$ and variance $\sigma_q^2 = 4\sigma^2(\lambda_\theta + \lambda_\phi + 2\sigma^2)$ to obtain

$$\begin{aligned} P_{\text{fa}} &= \frac{1}{\sqrt{2\pi}\sigma_{\text{fa}}} \int_\tau^\infty e^{-q^2/2\sigma_{\text{fa}}^2} dq = 1 - Q(\tau/\sigma_{\text{fa}}) \\ &= 1 - Q\left(\frac{M-1}{M} \sqrt{\frac{P_k}{N_0 B}} \Big/ \sqrt{1 + \frac{N_0 B}{2P_k M^2}} \right) \end{aligned} \tag{28}$$

$$\begin{aligned} P_D &= \frac{1}{\sqrt{2\pi}\sigma_D} \int_\tau^\infty e^{-(q-\mu_D)^2/2\sigma_D^2} dq \\ &= 1 - Q[(\tau - \mu_D)/\sigma_D] \\ &= Q\left(\frac{(M-1)}{\sqrt{(M-1)^2+1}} \sqrt{\frac{P_k}{N_0 B}} \Big/ \right. \\ &\qquad \left. \sqrt{1 + \frac{N_0 B}{2P_k[(M-1)^2+1]}} \right) \end{aligned} \tag{29}$$

where $\sigma_{\text{fa}}^2 \cong 8\sigma^2(2P_k M^2 + \sigma^2), \mu_D \cong 8(M-1)P_k, \sigma_D^2 \cong 8\sigma^2(2P_k[(M-1)^2+1] + \sigma^2)$, and the standard Gaussian distribution function is

$$Q(z) = \frac{1}{\sqrt{2\pi}} \int_{-\infty}^z e^{-x^2/2}\, dx. \tag{30}$$

The false-alarm rate is plotted in Fig. 5 for a 36-element array. Observe that a false-alarm rate of 10^{-6} requires a signal-to-noise power of approximately 13 dB. Use of (29) indicates a probability of detection in excess of 99%.

VI. A/D Converter Range and Resolution

The quantization step size of the analog-to-digital (A/D) converter must be sufficiently small to measure the smallest voltage change that will occur at the output of the detector. The smallest voltage change that is measured is the difference between the $\bar{q}_{90}$ and $\bar{q}_{270}$ signals (17)

$$\Delta q_{\text{RF}} = \bar{q}_{90} - \bar{q}_{270} = 4(M-1)a_k^2 \sin\delta. \tag{31}$$

To cover the range of the possible inputs, the ratio of the A/D converter full-scale reading to that of its least significant bit must be greater than or equal to the ratio of the full-scale voltage to the minimum detectable voltage step. The full-scale voltage is proportional to the peak RF power

$$P_{\text{PEAK}} \approx M^2 a_k^2 \tag{32}$$

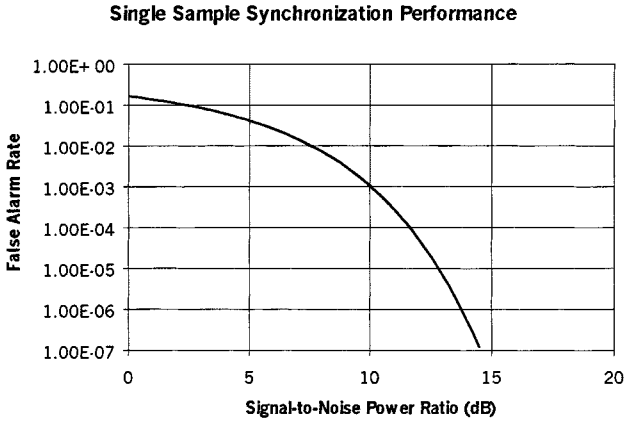

Fig. 5. Synchronization pulse false alarm rate.

so the minimum number of bits to detect a change of δ in the phase of a single element in the absence of noise is

$$B_{\min} = \log_2\left(\frac{P_{\rm PEAK}}{\Delta P_{\rm RF}}\right) = \log_2\left[\frac{M^2}{4(M-1)\sin\delta}\right]. \quad (33)$$

The required minimum number of bits for a measurement resolution of $\delta = 2°$ for a 36-element array is 8.05. However, the signal-to-quantization-noise ratio must be at least 10 dB greater than the signal-to-noise-power ratio to preclude degradation from quantization. For a peak loaded A/D converter, this ratio is approximately 6.02 $B+$ 1.77 dB, so that 8 bits is almost 40 dB above the signal-to-noise-power ratio.

VII. Calibration Time

The sample interval of T_s must be chosen according to the Nyquist criterion relative to the input filter bandwidth, and the filter bandwidth must be chosen to limit the input noise while passing the desired signal. From Fig. 2 the total time for calibration is

$$T_{\rm CAL} = 16N_{\rm SEQ}[2+M]T_{\rm PW} \quad (34)$$

where the pulse width may be taken as T_s, the number of array elements is M, and the number $N_{\rm SEQ}$ is the total number of phase sequences in the calibration procedure.

VIII. Imperfect Phase and Amplitude Control

The derivation of the phase and amplitude estimators in (19) and (20) assumes perfect amplitude and phase control of the element signal.The in-phase and quadrature components of this signal were denoted by $v_c(\theta)$ and $v_s(\theta)$ following (3). Actual phase shifters are unlikely to give exact phase settings of 0°, 90°, 180°, and 270°, and real attenuators may not permit exact control of the amplitude a_k. However, errors in the settings are deterministic and may be measured. Denote the phase settings of the kth element by $\theta_m = m\pi/2, m = 0,1,2,3$ with corresponding signal components

$$v_c = a_{km}\cos(\theta_m + \zeta_{km} + \delta_k)$$
$$v_s = a_{km}\sin(\theta_m + \zeta_{km} + \delta_k)$$

having amplitudes a_{km} and phase offsets ζ_{km} which contain imperfections and amplitude errors. Following the same rationale that led to (17) and (18) gives

$$\begin{aligned} E\{q_m - q_n\} &= a_{km}^2 - a_{kn}^2 + 2A_c[a_{km}\cos(\theta_m + \zeta_{km} + \delta_k) \\ &\quad - a_{kn}\cos(\theta_n + \zeta_{kn} + \delta_k)] \\ &\quad + 2A_s[a_{km}\sin(\theta_m + \zeta_{km} + \delta_k) \\ &\quad - a_{kn}\sin(\theta_n + \zeta_{kn} + \delta_k)] \end{aligned} \quad (35)$$

where

$$A_c = \sum_{\substack{\ell=1 \\ \ell\neq k}}^{M} a_{\ell,0}\cos(\zeta_{\ell,0} + \delta_\ell)$$
$$A_s = \sum_{\substack{\ell=1 \\ \ell\neq k}}^{M} a_{\ell,0}\sin(\zeta_{\ell,0} + \delta_\ell).$$

Evaluation of (35) at $\theta_m = 270°$ and $\theta_n = 90°$ yields

$$\begin{aligned} \bar{q}_{270} - \bar{q}_{90} &= a_{270}^2 - a_{90}^2 + [2A_c(a_{270}\sin\zeta_{270} + a_{90}\sin\zeta_{90}) \\ &\quad - 2A_s(a_{270}\cos\zeta_{270} + a_{90}\cos\zeta_{90})]\cos\delta_k \\ &\quad + [2A_c(a_{270}\cos\zeta_{270} + a_{90}\cos\zeta_{90}) \\ &\quad + 2A_s(a_{270}\sin\zeta_{270} + a_{90}\sin\zeta_{90})]\sin\delta_k \end{aligned} \quad (36)$$

and similarly for $\theta_m = 0°$ and $\theta_n = 180°$

$$\begin{aligned} \bar{q}_0 - \bar{q}_{180} &= a_0^2 - a_{180}^2 + [2A_c(a_0\cos\zeta_0 + a_{180}\cos\zeta_{180}) \\ &\quad + 2A_s(a_0\sin\zeta_0 + a_{180}\sin\zeta_{180})]\cos\delta_k \\ &\quad - [2A_c(a_0\sin\zeta_0 + a_{180}\sin\zeta_{180}) \\ &\quad - 2A_s(a_0\cos\zeta_0 + a_{180}\cos\zeta_{180})]\sin\delta_k. \end{aligned} \quad (37)$$

The subscript k indicating the element has been omitted on the amplitude and phase variations and on the power measurements $\bar{q}$ for simplicity in (36) and (37) since this dependence is understood. These expressions may be written as

$$\begin{aligned} (\bar{q}_{270} - a_{270}^2) - (\bar{q}_{90} - a_{90}^2) &= C_{11}\cos\delta_k + C_{12}\sin\delta_k \\ (\bar{q}_0 - a_0^2) - (\bar{q}_{180} - a_{180}^2) &= C_{21}\cos\delta_k + C_{22}\sin\delta_k \end{aligned} \quad (38)$$

with

$$\begin{aligned} C_{11} &= 2A_c(a_{270}\sin\zeta_{270} + a_{90}\sin\zeta_{90}) \\ &\quad - 2A_s(a_{270}\cos\zeta_{270} + a_{90}\cos\zeta_{90}) \\ C_{12} &= 2A_c(a_{270}\cos\zeta_{270} + a_{90}\cos\zeta_{90}) \\ &\quad + 2A_s(a_{270}\sin\zeta_{270} + a_{90}\sin\zeta_{90}) \\ C_{21} &= 2A_c(a_0\cos\zeta_0 + a_{180}\cos\zeta_{180}) \\ &\quad + 2A_s(a_0\sin\zeta_0 + a_{180}\sin\zeta_{180}) \\ C_{22} &= -2A_c(a_0\sin\zeta_0 + a_{180}\sin\zeta_{180}) \\ &\quad + 2A_s(a_0\cos\zeta_0 + a_{180}\cos\zeta_{180}). \end{aligned}$$

The equations in (38) are easily solved for δ_k to obtain the estimate as shown in (39) at the bottom of the page where the amplitudes a_m and phase offsets ζ_m are from measurements. Solution of the linear equations following (38) for the amplitude estimates gives

$$\begin{aligned}
\hat{a}_0 &= [C_{22}(A_c\cos\zeta_{180} + A_s\sin\zeta_{180}) \\
&\quad + C_{21}(A_c\sin\zeta_{180} - A_s\cos\zeta_{180})]/2 \\
&\quad \times [(A_c\cos\zeta_0 + A_s\sin\zeta_0) \\
&\quad \times (A_c\sin\zeta_{180} - A_s\cos\zeta_{180}) \\
&\quad - (A_c\sin\zeta_0 - A_s\cos\zeta_0) \\
&\quad \times (A_c\cos\zeta_{180} + A_s\sin\zeta_{180})] \\
\hat{a}_{180} &= -[C_{22}(A_c\cos\zeta_0 + A_s\sin\zeta_0) \\
&\quad + C_{21}(A_c\sin\zeta_0 - A_s\cos\zeta_0)]/2 \\
&\quad \times [(A_c\cos\zeta_0 + A_s\sin\zeta_0) \\
&\quad \times (A_c\sin\zeta_{180} - A_s\cos\zeta_{180}) \\
&\quad - (A_c\sin\zeta_0 - A_s\cos\zeta_0) \\
&\quad \times (A_c\cos\zeta_{180} + A_s\sin\zeta_{180}) \\
\hat{a}_{90} &= [C_{11}(A_c\cos\zeta_{270} + A_s\sin\zeta_{270}) \\
&\quad - C_{12}(A_c\sin\zeta_{270} - A_s\cos\zeta_{270})]/2 \\
&\quad \times [(A_c\sin\zeta_{90} - A_s\cos\zeta_{90}) \\
&\quad \times (A_c\cos\zeta_{270} + A_s\sin\zeta_{270}) \\
&\quad - (A_c\cos\zeta_{90} + A_s\sin\zeta_{90}) \\
&\quad \times (A_c\sin\zeta_{270} - A_s\cos\zeta_{270})] \\
\hat{a}_{270} &= -[C_{11}(A_c\cos\zeta_{90} + A_s\sin\zeta_{90}) \\
&\quad - C_{12}(A_c\sin\zeta_{90} - A_s\cos\zeta_{90})]/2 \\
&\quad \times [(A_c\sin\zeta_{90} - A_s\cos\zeta_{90}) \\
&\quad \times (A_c\cos\zeta_{270} + A_s\sin\zeta_{270}) \\
&\quad - (A_c\cos\zeta_{90} + A_s\sin\zeta_{90}) \\
&\quad \times (A_c\sin\zeta_{270} - A_s\cos\zeta_{270})]. \qquad (40)
\end{aligned}$$

It must be emphasized that the estimators (39) and (40) for the phase and amplitude variations are not closed-form expressions since the coefficients $C_{11}, C_{12}, C_{21}, C_{22}, A_c$, and A_s depend on these variations. Hence, the estimates must be solved by an iterative procedure. Further, observe that since there are power measurements $\bar{q}$ at four phase settings for each element, there are $4M$ data measurements. Since the estimators $\hat{\delta}_k$ and $\hat{a}_{km}$ constitute a set of $5M$ variables, the estimator equations given by (39) and (40) are dependent. This problem is circumvented by use of (20) for initial amplitude estimates. Equation (19) can be used for initial phase error estimates with (38) and (39) used for iteration of the phase error.

A program was written to implement and to verify the calibration procedure. The program generates the power measurements with Gaussian noise and assumes known values for the phase offsets ζ_{km} and ideal values $\hat{a}'_k$ for the initial amplitude estimates for each element. Using the power measurements $\bar{q}_{km}$ and (19), the program computes initial phase error estimates

$$\hat{\delta}_k^{(0)} = \tan^{-1}\left(\frac{\bar{q}_{k,270} - \bar{q}_{k,90}}{\bar{q}_{k,0} - \bar{q}_{k,180}}\right)$$

initial values for the signal sums (35) for each element

$$A_{c,k}^{(0)} = \sum_{\substack{\ell=1 \\ \ell\neq k}}^{M} \hat{a}'_\ell \cos\left(\zeta_{\ell,0} + \hat{\delta}_\ell^{(0)}\right)$$

and

$$A_{s,k}^{(0)} = \sum_{\substack{\ell=1 \\ \ell\neq k}}^{M} \hat{a}'_\ell \sin\left(\zeta_{\ell,0} + \hat{\delta}_\ell^{(0)}\right)$$

and amplitude estimates (20)

$$\hat{a}_k = \frac{\sqrt{(\bar{q}_{k,270} - \bar{q}_{k,90})^2 + (\bar{q}_{k,0} - \bar{q}_{k,180})^2}}{4A_{c,k}^{(0)}}.$$

The program iterates to compute the next values of the signal sums

$$A_{c,k}^{(i+1)} = \sum_{\substack{\ell=1 \\ \ell\neq k}}^{M} \hat{a}_\ell \cos\left(\zeta_{\ell,0} + \hat{\delta}_\ell^{(i)}\right)$$

and

$$A_{s,k}^{(i+1)} = \sum_{\substack{\ell=1 \\ \ell\neq k}}^{M} \hat{a}_\ell \sin\left(\zeta_{\ell,0} + \hat{\delta}_\ell^{(i)}\right)$$

the coefficients (38)

$$\begin{aligned}
C_{k,11}^{(i)} &= 2\hat{a}_k\left[A_{c,k}^{(i)}(\sin\zeta_{k,270} + \sin\zeta_{k,90})\right. \\
&\quad \left. - A_{s,k}^{(i)}(\cos\zeta_{k,270} + \cos\zeta_{k,90})\right] \\
C_{k,12}^{(i)} &= 2\hat{a}_k\left[A_{c,k}^{(i)}(\cos\zeta_{k,270} + \cos\zeta_{k,90})\right. \\
&\quad \left. + A_{s,k}^{(i)}(\sin\zeta_{k,270} + \sin\zeta_{k,90})\right] \\
C_{k,21}^{(i)} &= 2\hat{a}_k\left[A_{c,k}^{(i)}(\cos\zeta_{k,0} + \cos\zeta_{k,180})\right. \\
&\quad \left. + A_{s,k}^{(i)}(\sin\zeta_{k,0} + \sin\zeta_{k,180})\right] \\
C_{k,22}^{(i)} &= 2\hat{a}_k\left[-A_{c,k}^{(i)}(\sin\zeta_{k,0} + \sin\zeta_{k,180})\right. \\
&\quad \left. + A_{s,k}^{(i)}(\cos\zeta_{k,0} + \cos\zeta_{k,180})\right]
\end{aligned}$$

$$\hat{\delta}_k = \tan^{-1}\left(\frac{C_{11}\left[\left(\bar{q}_0 - a_0^2\right) - \left(\bar{q}_{180} - a_{180}^2\right)\right] - C_{21}\left[\left(\bar{q}_{270} - a_{270}^2\right) - \left(\bar{q}_{90} - a_{90}^2\right)\right]}{C_{22}[(\bar{q}_{270} - a_{270}^2) - (\bar{q}_{90} - a_{90}^2)] - C_{12}\left[(\bar{q}_0 - a_0^2) - (\bar{q}_{180} - a_{180}^2)\right]}\right) \qquad (39)$$

and the phase errors (39)

$$\hat{\delta}_k^{(i)} = \tan^{-1}\Big(\Big\{C_{k,11}^{(i)}[\bar{q}_{k,0} - \bar{q}_{k,180}] - C_{k,21}^{(i)}[\bar{q}_{k,270} - \bar{q}_{k,90}]\Big\}\Big/ \Big\{C_{k,22}^{(i)}[\bar{q}_{k,270} - \bar{q}_{k,90}] - C_{k,12}^{(i)}[\bar{q}_{k,0} - \bar{q}_{k,180}]\Big\}\Big).$$

The iteration continued until the estimates $\hat{\delta}_k^{(i)}$ converged within specified limits of the previous estimates $\hat{\delta}_k^{(i-1)}$.

The iterative procedure converged differentially within two or three iterations as expected since the derivative of the arctangent is less than unity and the array and electronics should have small variations. However, absolute convergence of the process was dependent on the signal-to-noise ratio and the number of samples.

To corroborate the results in (38)–(40), these generalizations should reduce to the previous expressions (19) and (20) under assumptions of small or negligible errors. Simplification of (35) as in the previous section obtains

$$\begin{aligned}\bar{q}_m - \bar{q}_n \cong\, & a_{km}^2 - a_{kn}^2 \\ & + 2A_c[a_{km}\cos(\theta_m + \zeta_m)\cos\delta_k \\ & \quad - a_{km}\sin(\theta_m + \zeta_m)\sin\delta_k \\ & \quad - a_{kn}\cos(\theta_n + \zeta_n)\cos\delta_k \\ & \quad + a_{kn}\sin(\theta_n + \zeta_n)\sin\delta_k] \end{aligned} \tag{41}$$

with the assumption $A_s \cong 0$. Writing the amplitude variations with phase as $a_{km} - a_{kn} = \varepsilon_{mn}$, noting $\theta_n = \theta_m + \pi$, and ignoring terms higher than first order, i.e., $\varepsilon^2, \varepsilon\cos\zeta, \varepsilon\sin\zeta$, etc., obtains

$$\begin{aligned}&\bar{q}_m - \bar{q}_n \\ &\quad \cong 2a_k\varepsilon_{mn} \\ &\qquad + 2a_k A_c[\cos\delta_k\{\cos(\theta_m + \zeta_m) - \cos(\theta_n + \zeta_n)\} \\ &\qquad - \sin\delta_k\{\sin(\theta_m + \zeta_m) - \sin(\theta_n + \zeta_n)\}] \\ &\quad = 2a_k\{\varepsilon_{mn} + A_c[\cos\delta_k\{\cos(\theta + \zeta_m) + \cos(\theta + \zeta_n)\} \\ &\qquad - \sin\delta_k\{\sin(\theta + \zeta_m) + \sin(\theta + \zeta_n)\}]\}. \end{aligned} \tag{42}$$

For $\theta = \theta_0 = 0$ or $\theta = \theta_{\pi/2} = \pi/2$, the analogous results to (17) and (18) are

$$\bar{q}_{270} - \bar{q}_{90} \cong 2a_k[2A_c\sin(\zeta + \delta_k) - \varepsilon] \tag{43}$$

$$\bar{q}_0 - \bar{q}_{180} \cong 2a_k[\varepsilon + 2A_c\cos(\zeta + \delta_k)] \tag{44}$$

with $\zeta \cong \zeta_m \cong \zeta_n$ the nominal phase, a_k the nominal amplitude, and $\sin\zeta_m \cong 0$ and $\sin\zeta_n \cong 0$. This simplification is tantamount to assuming that the imperfections for each element are uniform over the various phase settings. With this assumption the estimators from (39) and (40) reduce to

$$\hat{\delta}_k = \tan^{-1}\left(\frac{\bar{q}_{270} - \bar{q}_{90} + 2a_k\varepsilon_{270}}{\bar{q}_0 - \bar{q}_{180} - 2a_k\varepsilon_0}\right) - \zeta \tag{45}$$

$$\hat{a}_k = \frac{\sqrt{(\bar{q}_{270} - \bar{q}_{90} + 2a_k\varepsilon_{270})^2 + (\bar{q}_0 - \bar{q}_{180} - 2a_k\varepsilon_0)^2}}{4A_c}. \tag{46}$$

These results (45) and (46), which include imperfections in phase and amplitude control, are easily observed to reduce to the results for exact control given in (19) and (20) when there are no errors, i.e., $\varepsilon = 0$ and $\zeta = 0$.

IX. The Calibration Process

The phase error $\hat{\delta}_k$ and the amplitude error $\hat{a}_k$ for each element from (45) and (46) contain not only the errors attributable to the electronics but also any errors induced by attitude control or pointing of the antenna platform. Examination of the array factor of the antenna [3]

$$\begin{aligned} f(\theta,\varphi) &= \sum_{m,n} s_{mn} e^{jk\hat{\underline{r}}\cdot\underline{d}_{mn}} = \sum_{m=0}^{M-1}\sum_{n=0}^{N-1} \alpha_{mn} e^{jk(\hat{\underline{r}} - \hat{\underline{r}}_0)\cdot\underline{d}_{mn}} \\ &= \sum_{m=0}^{M-1}\sum_{n=0}^{N-1} \alpha_{mn} e^{jk(d_{x,m}\gamma + d_{y,n}\chi)} \end{aligned} \tag{47}$$

with $\gamma = \sin\theta\cos\varphi - \sin\theta_0\cos\varphi_0$ and $\chi = \sin\theta\sin\varphi - \sin\theta_0\sin\varphi_0$ reveals that any phase error that affects the phases of all elements equally will not affect the directivity of the antenna. In addition, random errors [4] with correlation times greater than the time for calibration and systematic errors that are invariant over the calibration period are inconsequential. However, systematic and random pointing errors of sufficiently short duration to affect calibration must be addressed if they affect individual elements differently. To the extent that the systematic errors or the means of random errors can be determined, these must be deducted from the measured errors $\hat{\delta}_k$ and $\hat{a}_k$ to give corrected estimates $\tilde{\delta}_k$ and $\tilde{\alpha}_k$. Any residual pointing errors that cannot be estimated must be resolved by iteration of the calibration procedure.

For a given calibration measurement, the beam of the antenna is pointed using the previously determined corrections C_δ for the phase and C_a for the amplitude. Given the corrected estimates $\tilde{\delta}_k$ and $\tilde{\alpha}_k$ of the phase and amplitude errors, a phase correction C'_δ and an amplitude correction C'_a may be computed recursively from the previous corrections by

$$C'_\delta = C_\delta - \mu_\delta\delta_k \tag{48}$$

$$C'_a = C_a - \mu_a\alpha_k \tag{49}$$

where α_k is the ratio of the measured power $\hat{a}_k^2/2$ to the nominal power P_k for the kth element. The scaling factors μ_δ and μ_a should be less than unity to insure convergence, and the calibration and amplitude correction adjustment must be performed iteratively until acceptable accurracy is achieved. As noted previously, the adjustment must be done after calibrating the entire array since adjusting any element will change the reference point for all other elements.

The calibration process is relatively simple, as indicated by an example involving an array on a communication satellite. Calibration may be invoked as a diagnostic measure either in response to reduced or anomalous performance or as a periodic component of satellite operations. Fig. 6 shows the systems for transmit (forward link) and receive (return link) calibration. In either case, a signal flows through the array on a beam that is

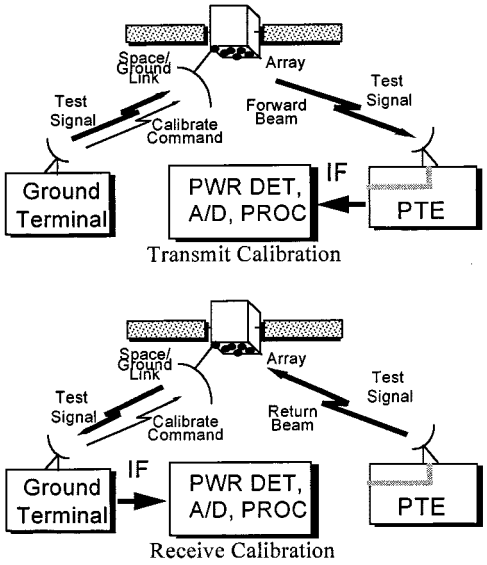

Fig. 6. Array calibration on satellite.

not in service, and the electronics is commanded to perform the phase sequence after pointing at a ground station. Note that any automatic gain control or channel control must be inoperative during the calibration process. Detection and calibration are performed at the ground station. This calibration procedure is repeated until the phase and amplitude errors of the array elements converge within acceptable limits.

Given the phase and amplitude corrections for the forward and return arrays, the decision process for updating phase corrections is complex. Calibration measurements may be repeated to corroborate results or to ameliorate the contributions of pointing errors, and errors that are below the accuracy of the calibration system may be ignored. Errors that are significant relative to the calibration accuracy but small relative to the resolution of the phase shifters may require attention, and errors that are comparable to or greater than the resolution of the phase shifters need address. Systematic errors that are not uncommon in manufacture can be accomodated by introduction of rules or procedures since their nature is not random.

X. Summary

Calibration of a phased array may be accomplished remotely with very little overhead to the service of the antenna. Cycling of the phases of elements through only four orthogonal phases reduces significantly the time for calibration, and use of a maximum likelihood algorithm gives optimal accuracy. Good performance and convergence are obtained for reasonable signal-to-noise ratios and sample sizes.

References

[1] T. Katagi, Y. Konishi, Y. Tamai, and Y. Iida, "A large deployable active phased array antenna for satellite use," in *Proc. Amer. Inst. Aeronautics and Astronautics*, AIAA-94-1070-CP, 1994, pp. 1075–1084.

[2] R. Sorace, V. Reinhardt, and C. Chan, "Phased array caliberation by Orthogonal phase sequence,", Jan. 19, 1999.

[3] R. E. Collin and F. J. Zucker, *Antenna Theory*. New York: McGraw-Hill, 1969, pt. 1, ch. 5.

[4] M. I. Skolnik, *Radar Handbook.*. New York: McGraw-Hill, 1970, ch. 9.

Ron Sorace (M'80–SM'85) received the B.S. degree in mathematics and the M.S. degree in physics from the University of Maryland, College Park, in 1968 and 1974, respectively, and the Ph.D. degree in engineering from the University of California, Los Angeles, in 1981.

He has more than 30 years of experience in the aerospace and satellite communications industries. He is with Boeing Space Systems, formerly Hughes Space and Communications Co., Los Angeles, since 1986. His interests include detection, modulation, antennas, propagation and scattering, radar, orbital studies, microwave electronics, and signal processing.